

PACS numbers: 07.85.Tt; 52.50.Jm
DOI: 10.1070/QE2011v041n03ABEH014293

Four-channel X-ray microscope for plasma investigations on the Sokol-P laser facility

D.A. Vikhlyaev, D.S. Gavrilov, A.G. Kakshin, A.V. Potapov, K.V. Safronov

Abstract. **The design, assembly, and alignment of a Kirkpatrick–Baez X-ray microscope are described. A technique for the experimental evaluation of the resolving power of the microscope is outlined. This microscope permits obtaining simultaneous images of laser target plasmas in narrow energy regions belonging to the 0.3–1.5-keV X-ray range with a resolution of ~2 μm.**

Keywords: *X-ray microscopy of laser-produced plasma, Kirkpatrick–Baez scheme.*

1. Introduction

Spatially resolved X-ray plasma radiation measurements provide important information about the processes occurring in the heating of targets by laser radiation.

On the Sokol-P laser facility, two-dimensional X-ray images of laser target plasmas are recorded with the aid of a pinhole camera. This is the simplest optical device which permits obtaining the images of objects [1, 2]. The pinhole camera resolution is defined by the formula [3]

$$\delta^2 \approx \left[\frac{D(\Gamma+1)}{\Gamma}\right]^2 + \left(\frac{2.44\lambda a}{D}\right)^2,$$

where λ is the wavelength; D is the pinhole diameter; a is the source–pinhole distance; and Γ is the magnification. Pinhole cameras provide distortion-free images and enable imaging objects in X-rays. However, it suffers from significant disadvantages [4]:

(i) the spatial resolution of a pinhole camera is limited by diffraction by the pinhole aperture;

(ii) when the resolution [5] is made as high as several micrometers, its luminosity becomes extremely low;

(iii) the width of its spectral window may not be narrower than several angstroms.

Furthermore, there is one more fundamental difficulty of using a pinhole camera on the Sokol-P facility: the strong background of hard X-ray radiation produced in the target, at the walls of the vacuum chamber, and at the structural elements of diagnostic instrumentation, including the pinhole camera itself, under bombardment by fast electrons. Since the pinholes which form the pinhole-camera image are made in a thin foil, technically it is rather difficult to suppress the background irradiation of photographic film by the hard X-ray radiation.

An instrument which makes it possible to achieve a higher spatial resolution (~1 μm) and is by far more complex in fabrication and alignment than a pinhole camera is an X-ray microscope [6–8]. The luminosity and spatial resolution of the X-ray microscope are much higher than for pinhole cameras.

The systems of spherical mirrors with crossed planes of radiation incidence, as applied to the problem of constructing a stigmatic X-ray microscope, were first considered by Kirkpatrick and Baez [6]. The microscope consists of two cylindrical (or spherical) mirrors whose reflecting surfaces intersect at a right angle. In this case, the rays reflected successively by the two mirrors at grazing incidence angles form the two-dimensional image of the radiating object, in accordance with the laws of geometrical optics. The presence of two mutually orthogonal mirrors is needed to cancel astigmatism, which emerges in a single reflection.

The aim of our work was to make an X-ray microscope operating in the 0.3–1.5 keV photon energy range. The resolution of the microscope had to be better than 2 μm, which is related to the decrease in the laser focal spot diameter to 6–7 μm, resulting from the amendment of the Sokol-P facility [9].

2. X-ray microscope design

The central angle of radiation incidence on the mirrors was selected at a value $\theta = 2°$, proceeding from the requisite spectral composition (E = 0.3–1.5 keV) of the radiation to be recorded. For $\theta > 3°$, the reflection coefficient for photon energies $E > 1$ keV is substantially lower. Meanwhile, recording 0.3–0.8-keV photons for $\theta < 1°$ will be hindered due to the higher contribution to the image made by $E > 1.5$-keV photons, because the photographic film responsivity to these photons is higher by a factor of several tens.

X-ray radiation selection was afforded by microscope mirrors and X-ray filters. In the soft X-ray radiation range of interest the best-suited materials for the mirrors are SiO_2, Ni, Mo, and Au, since they are void of absorption jumps and possess good reflection characteristics in this range.

The low-energy spectrum cutoff was effected by X-ray filters. Figure 1 shows the calculated spectral transmission functions of microscope channels [10], which were the products of filter transmission and mirror reflection coefficients.

In the recording of images with an X-ray microscope, the blackening density of photographic film depends on several factors, including the angular dimension of the entrance

D.A. Vikhlyaev, D.S. Gavrilov, A.G. Kakshin, A.V. Potapov, K.V. Safronov E.I. Zababakhin All-Russian Scientific-Research Institute of Technical Physics, Russian Federal Nuclear Centre, ul. Vasil'eva 13, 456770 Snezhinsk, Chelyabinsk region, Russia; e-mail: dep5@vniitf.ru

Received 10 February 2010; revision received 13 January 2011
Kvantovaya Elektronika **41** (3) 234–238 (2011)
Translated by E.N. Ragozin

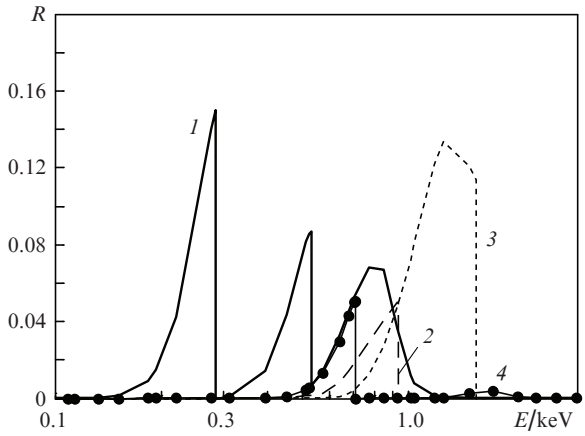

Figure 1. Spectral transmission functions of microscope channels consisting of two SiO_2 mirrors and a 2-μm-thick $C_{10}H_8O_4$ filter (*1*), SiO_2 and Mo mirrors and a 1-μm-thick Cu filter (*2*), two Mo mirrors and a 5.4-μm-thick Al filter (*3*), and two Ni mirrors and a 1.5-μm-thick Fe filter (*4*).

aperture of a channel. The minimal angular dimension $A_{\min}$ of the entrance aperture of the Kirkpatrick–Baez system is $\sim 4.5\times10^{-6}$ sr. This value corresponds to the diffraction-limited (the highest possible) resolution δ_d = 2–0.4 μm (E = 0.3–1.5 keV). For comparison: the angular dimension A_{obs} of the pinhole camera employed in experiments on the Sokol-P laser facility is equal to $\sim10^{-7}$ sr. This pinhole camera aperture permits obtaining X-ray plasma images with a good blackening density of the photographic film. Unlike the pinhole camera, the X-ray microscope has mirrors, which attenuate the flux of photons with energies $E > 0.8$ keV by factors of three-to-five, the entrance aperture of a microscope channel must exceed fivefold A_{obs}. In our case, $A_{\min}$ exceeds A_{obs} by a factor of 50, making it possible to safely record the images of the luminous target domain. The initial parameters for X-ray microscope design are given below.

Target–primary mirror distance a/mm	50
Mirror spacing Δ/mm	6
Incidence angle θ/deg	2
Magnification Γ	6–9
Resolution (in the object plane) δ/μm	2
Wavelength λ/Å of the radiation recorded	8–45

The target–primary mirror separation a was selected proceeding from the dimensions of the laser beam and the feasibility of installing other diagnostic equipment, and the mirror spacing Δ (equal to the width of the mirror or greater) was preliminarily estimated from $A_{\min}$.

The system of spherical mirrors with crossed planes of radiation incidence, which was proposed by Kirkpatrick and Baez, is schematised in Fig. 2. Mirror M1 produces the astigmatic source image – meridional at point O′ and sagittal at point O″. The radius of curvature and position of mirror M2 should be such that the image at point O′ is sagittal and at point O″ meridional for point O_1, at which there forms the stigmatic image of the source O, according to the law of reversibility [8].

On this basis one may write the following system of equations

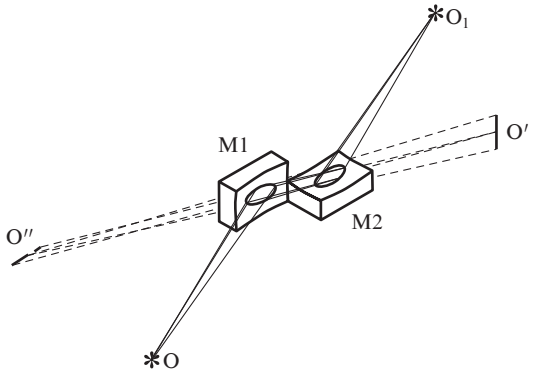

Figure 2. Schematic diagram of the Kirkpatrick–Baez microscope.

$$\frac{1}{f_{m1}} = \frac{1}{b_{m1}} + \frac{1}{a},$$

$$\frac{1}{f_{s2}} = \frac{1}{b_{m1} - \Delta} + \frac{1}{\Gamma_1 a},$$

$$\frac{1}{f_{s1}} = \frac{1}{b_{s1}} + \frac{1}{a}, \qquad (1)$$

$$\frac{1}{f_{m2}} = \frac{1}{b_{s1} - \Delta} + \frac{1}{\Gamma_2 a},$$

where $f_{s1,s2} = R_{1,2}/(2\sin\theta)$ and $f_{m1,m2} = (R_{1,2}\sin\theta)/2$ are the sagittal and meridional focal lengths, respectively; $R_{1,2}$ are the radii of curvature of the mirrors; Γ_1 and Γ_2 are the system's magnifications in the sagittal and meridional planes, respectively; b_{m1} and b_{m2} are the distances of the centre of the primary mirror from points O′ and O′, respectively.

By solving the system of equations (1) and assuming, in the first approximation, $\Gamma_1 = \Gamma_2 = \Gamma = 7$, we obtain $R_1 \approx 2515$ mm and $R_2 \approx 2770$ mm. The tooling of our optical workshop enables fabricating a series of mirrors of K8 glass with a surface roughness of a few angstroms and radii close to the calculated ones. By way of aberration simulations performed with the aid of OPAL-PC code package it was determined that mirrors with the radii of curvature $R_1 = 2582$ mm, $R_2 = 2858$ mm of this series afford the highest microscope resolution. The calculated data are given below.

Mirror width/mm	4
Target–primary mirror distance a_1/mm	50
Detector–secondary mirror distance b_2/mm	450
Entrance aperture/sr	7×10^{-6}
Magnification Γ_1 in the sagittal plane	9
Magnification Γ_2 in the meridional plane	8.18
Resolution at the centre of the object field δ/μm	~1.5
Wavelength λ/Å of the radiation recorded	8–45

The entrance aperture of the system complies with the limitations imposed above: it is a rectangle measuring 140×125 μm (at the centre of the primary mirror). The anamorphism factor A, which accounts for the difference in magnification, is equal to 1.1.

The same resolution δ throughout the photon energy range is caused by aberrations (coma and spherical aberra-

tion). Their elimination calls for the employment of aspherically shaped mirrors, which are difficult to fabricate. In our case, the calculated resolution is no worse than the desired one, which allows the application of simple spherical mirrors. For points at the edge of an object of radius ~ 30 μm, the calculated resolution is no worse than ~ 2 μm.

3. X-ray microscope assembly

The X-ray microscope objective consists of four optically equivalent channels [7] formed by two pairs of spherical mirrors (Fig. 3). Each objective channel has a reflective coating of its own (see Fig. 1). The placement of the corresponding X-ray filters after the mirrors enables recording images simultaneously in four spectral channels in one laser shot. For an incidence angle $\theta = 2°$, the spacing of the surfaces of the pair of mirrors closest to the object is $2d_x = 3.5$ mm and the spacing of the surfaces of the second pair of mirrors is $2d_y = 3.9$ mm.

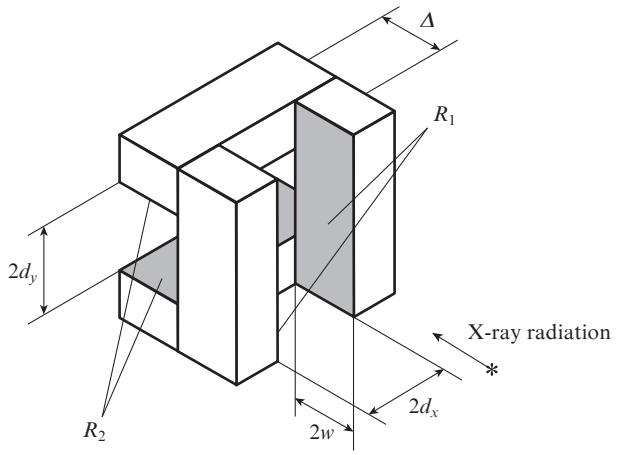

Figure 3. Four-channel X-ray microscope objective.

The four-channel X-ray microscope objective was assembled on an optical stand with the aid of a He–Ne laser (*1*) (Fig. 4). The light beam passes through a microlens (*3*), comes to a focus and subsequently diverges. The angle of the diverging beam should exceed $2\sqrt{2}\theta$. The beam waist (*4*) measures a few micrometres in diameter and may therefore be treated as a point object. The position of the waist (*4*) in the object plane as well as the direction of the diverging beam are adjusted by deflecting mirrors (*2*). In the course of assembly, the relative position of microscope mirrors (*6*) is monitored with the aid of a screen (*8*), which is mounted at a long distance L from the microscope (in our case, $L = 1$ m). Preliminarily drawn on the screen (*8*) were reference lines, which indicated the positions of the rays that did not experience reflection and the rays reflected from the mirrors.

One of the principal conditions for correct operation of the microscope consists in the passage of its axis through the centre of the focal spot on the target. The position of the microscope axis relative to the centre of the focal spot is defined by a hard aperture (*9*). The direction of the microscope axis may be defined with an auxiliary mirror mounted perpendicular to the axis. The auxiliary semitransparent mirror was temporarily mounted on an adjustable stage (*10*) between the microscope mirrors (*6*) and the hard aperture (*9*). To this end, the microlens (*3*) is removed and, with the aid of mirrors (*2*), the laser beam is directed along the microscope axis through the centres of apertures (*5*, *7*), and (*9*).

A reference laser beam passing through the centre of the focal spot and the mounting flange of the microscope is introduced in the diagnostic chamber. After this, the microscope is placed in the chamber (Fig. 5). The fastener provides two transverse displacement with the help of screw (*1*), two angular displacement with the help of screw (*2*), as well as linear motion (adjustable distance *a*) along the axis of the microscope in the grooves of the supporting arm (*6*). With the adjustment screws (*1*) and (*2*) the axis of the microscope is combined with the axis of the reference laser beam. The auxiliary mirror is removed. Thus, a preliminary alignment of the X-ray microscope is achieved.

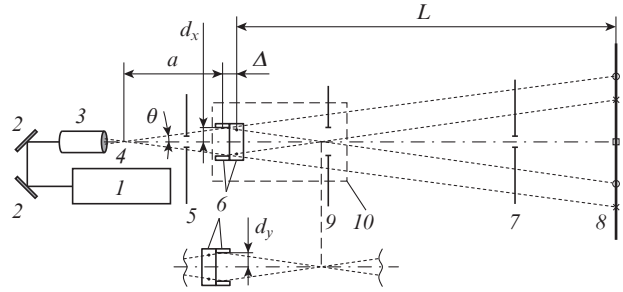

Figure 4. Schematic representation of the optical setup for assembling the four-channel objective of the X-ray microscope (see text for the notation).

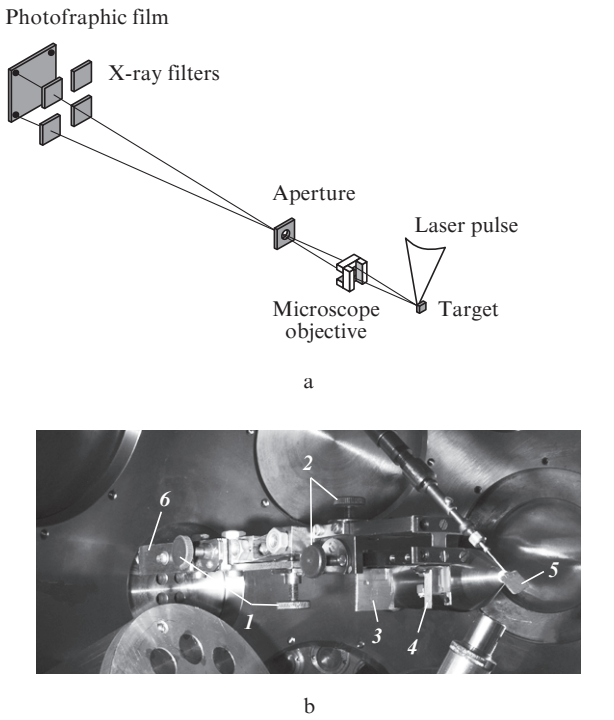

Figure 5. Schematic (a) and photograph (b) of an X-ray microscope: (*1*, *2*) adjusting screws; (*3*) aperture; (*4*) four-channel objective of the X-ray microscope; (*5*) target; (*6*) supporting arm.

The final alignment of the microscope is performed to achieve the symmetry of the picture on the screen with the help of adjusting screws (*1*). For this purpose, a laser beam that diverges from the centre of the focal spot is directed to the microscope. As a target, use is made of a mirror reflecting the adjusting (focused on the mirror surface) beam in the X-ray microscope.

4. Experimental evaluation of microscope resolution

Correct processing of the images recorded with the microscope calls for the knowledge of its resolution. Measuring this characteristic on the stationary X-ray KRUS-UKROP facility [11] (like in Ref. [7]) is fallacious because it relies substantially on alignment precision. Measurements on this facility would permit determining the best resolution, which may differ several-fold from the real one. It is therefore necessary to measure the resolution of the microscope in its operating position on the Sokol-P laser facility.

The microscope resolution was measured in the following way. In one of the series of experiments executed on the Sokol-P laser facility, use was made of a target design schematised in Fig. 6. The target was made of aluminium foil (*2*) glued to a copper fixture (*1*). One can see that the X-ray microscope (*4*) does not 'see' the entire radiating target domain (*3*), since a part of it is obscured by the copper fixture. From the sharp edge of the image of the radiating domain it is possible to determine the resolution of the microscope. The image recorded on Agfa Structurix D7 FW photographic film in one of experiments is shown in Fig. 7a. Figures 7b and 7c show the image of the radiating target domain and the densitogram of its sharp edge (boundary curve).

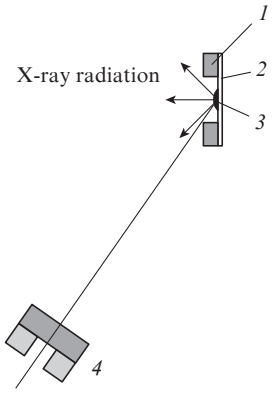

Figure 6. Experimental setup (see text for the notation).

The distance in the object plane corresponding to the fall-off of the boundary curve (Fig. 7c) is equal to ~ 5 μm. Aberration simulations for a point of the object located at a distance of 30 μm from its centre (Fig. 7b) suggest that this characteristic of the boundary curve is also equal to 5 μm. This corresponds to the design resolution of the microscope $\delta \approx 2$ μm. consequently, the real resolution of the microscope is no worse than 2 μm.

Shown for comparison in Fig. 8 are the images of the radiating target domain (in the ~ 1.5 keV energy region) recorded with the aid of the X-ray microscope and a pinhole camera

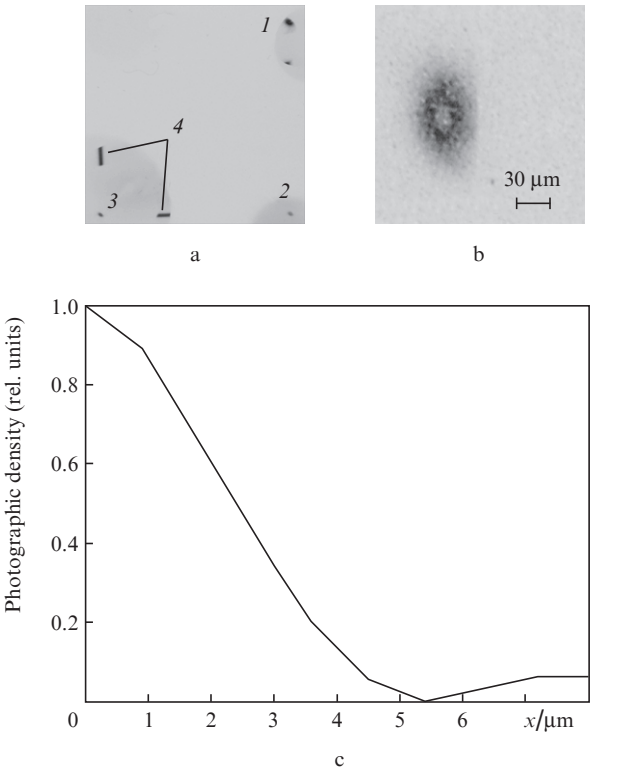

Figure 7. Images of the radiating target domain in the channels with photon energies of 0.3 (*1*), 0.9 (*2*), and 1.5 keV (*3*) (a), enlarged image in channel *3* (b), and densitogram of the sharp edge of the image in Fig. 7b (c); *4* – lines corresponding to the single reflection from the mirrors.

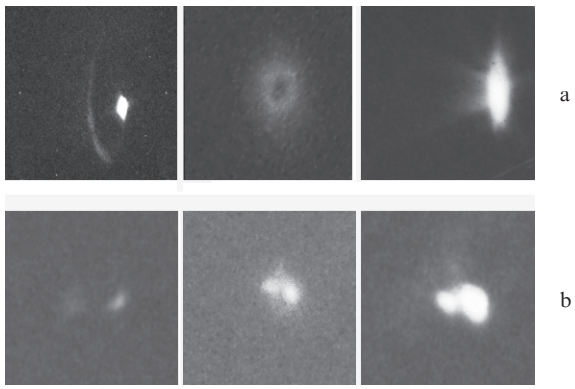

Figure 8. Images of the radiating domain of different targets obtained with the aid of the X-ray microscope (a) and a pinhole camera (b).

with a pinhole diameter of ~ 4 μm. One can see that the X-ray microscope affords clearer images than the pinhole camera.

5. Conclusions

A Kirkpatrick – Baez X-ray microscope was made for recording two-dimensional images of the radiating domain of laser targets on the Sokol-P laser facility. This microscope enables recording images with a ninefold magnification. Along with mirrors, use is made of X-ray filters, making it possible to simultaneously obtain images in four narrow regions in the 0.3 – 1.5 keV X-ray range. The microscope resolution was experimentally evaluated at $\delta \approx 2$ μm at the edge of the image,

which is in agreement with the design resolution. The calculated microscope resolution at the centre of the image is equal to ~1.5 μm. Therefore, the X-ray microscope will enable carrying out plasma investigations with a high spatial resolution.

References

1. Key M.H., Eidman K., Dorn C. *Phys. Lett. A*, **48**, 121 (1974).
2. Zakharenkov Yu.A., Zorev N.N., Krokhin O.N., et al. *Zh. Eksp. Teor. Fiz.*, **70**, 574 (1976).
3. Koch J.A., Landen O.L., Barbee T.W., et al. *Appl. Opt*., **37**, 1784 (1998).
4. Boiko V.A., Pikuz S.A., Faenov A.Ya. *Prib. Tekh. Eksp.*, (2), 5 (1980).
5. Landsberg G.S. *Optika* (Optics) (Moscow: Fizmatlit, 2003).
6. Kirkpatrick P., Baez A.V. *J. Opt. Soc. Am*., **38** (9), 766 (1948).
7. Seward F., Dent J., Boyle M., et al. *Rev. Sci. Instrum.*, **47** (4), 464 (1976).
8. Vinogradov A.V., Brytov I.A., Grudskii A.Ya., et al. *Zerkal'naya rentgenovskaya optika* (X-Ray Mirror Optics) (Leningrad: Mashinostroenie, 1989).
9. Andriyash A.V., Vikhlyaev D.A., Gavrilov D.S., et al. *Bull. Am. Phys. Soc.*, **53** (14), 153 (2008).
10. Henke B.L., Gullikson E.M., Davis J.C. *Atomic Data and Nuclear Data Tables* (Orlando: Academic Press, Inc., 1993, No. 2).
11. Ostashev V.I. *Effekt shepchushchei galerei v eksperimentakh s puchkami MRI* (Whispering-Gallery Effect in Experiments with Soft X-Ray Radiation Beams) (Snezhinsk: Izd. RFYaTs–VNIITF, 2008).